Inorg. Chem. **2004**, *43*, 4604–4609

Composition–Structure Relationships in Polar Intermetallics: Experimental and Theoretical Studies of $LaNi_{1+x}Al_{6-x}$ ($x = 0.44$)

Delphine Gout, Evan Benbow, Olivier Gourdon, and Gordon J. Miller*

Department of Chemistry and Ames Laboratory, U.S. Department of Energy, Iowa State University, Ames, Iowa 50011-3111

Received March 2, 2004

A new ternary aluminide, $LaNi_{1+x}Al_{6-x}$ ($x = 0.44$), has been synthesized from La, Ni, and Al in sealed silica tubes. Its structure, determined by single-crystal X-ray diffraction, is tetragonal *P4/mmm* (No. 123) with $Z = 1$ and has the lattice parameters $a = 4.200(8)$ and $c = 8.080(8)$ Å. Refinement based on F_0^2 yielded $R_1 = 0.0197$ and $wR_2 = 0.020$ [$I > 2\sigma(I)$]. The compound adopts a structure type previously observed in $SrAu_2Ga_5$ and $EuAu_2Ga_5$. The atomic arrangement is closely related to the one in $BaAl_4$ as well as in other rare-earth gallide compounds such as $LaNi_{0.6}Ga_6$, $HoCoGa_5$, $Ce_4Ni_2Ga_{20}$, $Ce_4Ni_2Ga_{17}$, Ce_4NiGa_{18}, and $Ce_3Ni_2Ga_{15}$. This structure exhibits a large open cavity which may be filled by a guest atom. Band structure calculations using density functional theory have been carried out to understand the stability of this new compound.

Introduction

Recently, the crystal structure of $Ce_4Ni_6Al_{23}$ has been determined and observed to show heavy fermion behavior, as in other cerium−nickel−aluminum compounds.[1] Our recent work on these cerium compounds shows that the Ce-4*f* orbitals play a role in these properties. Therefore, our research in the Al-rich portion of the lanthanum−nickel−aluminum system is motivated primarily as a comparison with the Ce analogues to substantiate the origin of heavy fermion behavior by the Ce-4*f* orbitals. In addition, we also study the possibility of inserting small atoms such as hydrogen or lithium in a La−Ni−Al framework. Indeed, numerous studies have been done in the La−Ni−Al system for possible hydrogen storage properties.[2]

With the goal of preparing $La_4Ni_6Al_{23}$ and studying its properties in comparison with $Ce_4Ni_6Al_{23}$, instead we discovered a new compound in the lanthanum−nickel−aluminum system, $LaNi_{1+x}Al_{6-x}$ ($x = 0.44$), and determined its structure by single-crystal X-ray diffraction. Unlike the cerium−nickel−aluminum system, which shows numerous phases, the corresponding ternary lanthanum system is very poorly characterized. To our knowledge only two phases are known in the Al-rich portion of this system: La_4NiAl_5[3] and compounds in the solid solution $La(Ni_{1-x}Al_x)_5$.[4] The structure of this new compound, closely related to the $BaAl_4$ structure type, is quite interesting because it exhibits a large open cavity in the center of the unit cell, which could be filled by a guest atom such as hydrogen or small alkali metals, e.g., lithium.

Experimental Section

General Synthesis. The title compound was prepared from the elements, lanthanum (ingots, Ames Laboratory, 99.99%), nickel (powder, Johnson Matthey, 99.997%), and aluminum (pellets, Aldrich, 99.99%) in the molar ratio La:Ni:Al = 4:6:23. The elements were arc melted under high purity argon on a water-cooled copper hearth. The weight loss during melting was less than 0.2%. The alloy was annealed at 1073 K in evacuated silica tubes for 10 days to improve the crystallinity and to obtain a sufficient size for single-crystal measurements. After cooling from 1073 to 673 K for 2 days and, thereafter, a natural cooling to room temperature of the closed furnace, the final product was obtained. These crystals are stable upon exposure to air and water. A microprobe analysis by energy-dispersive X-ray spectroscopy (EDS) performed on a Hitachi S-2460N ESEM gave the chemical formula $La_{4.0(1)}Ni_{5.8(1)}Al_{22.3(3)}$. To obtain the quantitative values, Al, Ni, and La_2O_3 were used as standards.

* Author to whom correspondence should be addressed. E-mail: gmiller@iastate.edu.

(1) Gout, D.; Benbow, E.; Gourdon, O.; Miller, G. J. *J. Solid State Chem.* **2003**, *174*, 471−481.
(2) Pyun, S.-I.; Han, J.-N.; Yang, T.-H. *J. Power Sources* **1997**, *65*, 9−13.
(3) Rikhal, R. M.; Aksel'rud, L. G.; Zarechnjuk, O. S. *Dopov. Akad. Nauk. Ukr. RSR Ser. A* **1981**, *43*(9), 86−90.
(4) Takeshita, T.; Malik, S. K.; Elattar, A. A.; Wallace, W. E. *AIP Conf. Proc.* **1976**, *34*, 230−232.

10.1021/ic0497331 CCC: $27.50
Published on Web 06/25/2004

Table 1. Structural and Crystallographic Data for $LaNi_{1.44}Al_{5.56}$

formula	$LaNi_{1.44}Al_{5.56}$
mol wt (g mol^{-1})	747.51
cryst syst	tetragonal
space group	*P*4/*mmm* (No. 123)
Z	1
cell parameters	$a = b = 4.189(2)$ Å
	$c = 8.032(3)$ Å
	$V = 140.94(5)$ Å^3
density calc (g cm^{-3})	17.608
temperature	293 K
radiation	$\lambda_{MoK-L2,3} = 0.71069$ Å
diffractometer	Siemens P4
angular range 2θ (°)	0−54
hkl range	$-5 \le h \le 5$
	$-5 \le k \le 5$
	$-9 \le l \le 9$
linear absorption coefficient (cm^{-1})	519.29
absorption correction	analytical
total recorded reflections	388
observed reflections (I>3σ(I))	383
Rint (%)	4.98
refinement	F^2
weighting scheme	$w = 1/\sigma^2\|F_o\|$
no. of refined parameters	14
refinement results	R(%) = 1.97/Rw(%) = 5.12
	GOF = 2.78
residual electronic density	[−1.19,+0.77] e$^-$/Å^3

Numerous syntheses under the same experimental conditions in an attempt to modify the Al/Ni ratio of $LaNi_{1+x}Al_{6-x}$ over the range of $x = 0-0.5$ did not yield any other phase than the title compound. However, X-ray powder patterns of the different products show small quantities of $LaAl_3$ and $LaAl_{4-x}$ ($BaAl_4$ structure type).

Crystal Structure Determination. Diffracted intensities were collected at room temperature with a Siemens P4 diffractometer. The entire set of reflections was consistent with tetragonal symmetry and could be indexed by a primitive lattice ($a \approx 4.0$ Å and $c \approx 8.0$ Å). The intensities of the reflections were adjusted for Lorentz polarization and corrected for absorption via a Gaussian analytical method, and the crystal shape and dimensions were optimized with the STOE X-Shape program[5] on the basis of equivalent reflections. All data treatments, refinement, and Fourier syntheses were carried out with the JANA2000 program package.[6] The reflection sets were averaged according to the 4/*mmm* point group, yielding internal *R* values of 4.93% for observed reflections ($I > 2\sigma(I)$) (see Table 1 for more information). All refinements were performed on F^2 with all reflections included, but the residual *R* factors are reported for observed reflections only.

A structural model for $\sim LaNi_{1.45}Al_{5.55}$, close to the chemical composition observed from EDS analysis, was established using direct methods (SIR97 program[7]). A first series of refinement cycles with isotropic displacement parameters yielded an *R*-value of 4.78% (7 parameters). At this stage of the refinement one of the two aluminum sites exhibited a negative displacement parameter. A mixed occupancy by nickel and aluminum was initiated on this site, which converged to an *R*-value of 2.70% for only one more parameter. Moreover, the displacement parameters of these atoms went back to positive values. The Ni/Al ratio on this site refines close to 22/78. Introduction of anisotropic displacement parameters and a secondary extinction coefficient (type I) led to $R = 1.97\%$ for 14 parameters. Two others crystals from the same sample have also been refined and give the same Ni/Al ratio within one standard deviation. Atomic positions and displacement parameters are listed in Tables 2 and 3. Interatomic distances are listed in Table 4.

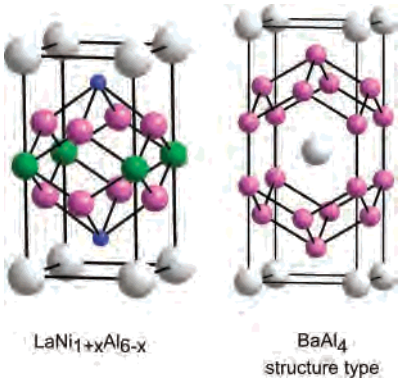

Figure 1. Unit cells of $LaNi_{1.44}Al_{5.56}$ and $BaAl_4$ structures. The gray, green, blue, and purple spheres represent, respectively, the La or Ba atoms, Ni atoms, mixed site of Ni/Al atoms, and Al atoms.

Table 2. Atomic Coordinates and Equivalent Isotropic Atomic Displacement Parameters of $LaNi_{1.44}Al_{5.56}$[a]

atom	Wyckoff position	*x*	*y*	*z*	ADP_{eq} (Å^2)
La	1a	0	0	0	0.80(2)
Ni	1b	0	0	1/2	0.80(3)
X	2h	1/2	1/2	0.1478(3)	0.87(5)
Al	4i	0	−1/2	0.6644(2)	1.15(5)

[a] X = 78.150(4)Al/21.850Ni.

Table 3. Anisotropic Atomic Displacement Parameters of $LaNi_{1.44}Al_{5.56}$[a]

atom	U_{11}	U_{22}	U_{33}
La	0.0095(5)	0.0095(5)	0.0116(6)
Ni	0.0098(6)	0.0098(6)	0.011(1)
X	0.011(1)	0.011(1)	0.011(1)
Al	0.020(1)	0.012(1)	0.012(1)

[a] $U_{12} = U_{13} = U_{23} = 0$.

Table 4. Selected Bond Distances (Å) in $LaNi_{1.44}Al_{5.56}$

La−X (×8)	3.1911(9)
La−Al (×8)	3.414(1)
Ni−Al (×8)	2.4760(8)
X−X	2.374(3)
X−Al (×4)	2.581(2)
Al−Al	2.641(2)
Al−Al (×4)	2.9620(7)

Structural Discussion. $LaNi_{1+x}Al_{6-x}$ ($x = 0.44$) crystallizes in a structure type which was observed in $EuAu_2Ga_5$ and $SrAu_2Ga_5$ by Cordier et al.[8] The structure is illustrated in Figure 1. By connecting the atoms of the (Ni, Al) network, the structure exhibits an empty rhombic dodecahedral site (RD) which is surrounded by La atoms. These RD share diamond faces that are perpendicular to the (*ab*) plane. This new structure is closely related to the $BaAl_4$ structure type as we can see in Figure 1. Such comparison may be understandable by the fact that $LaAl_{4-\delta}$[9] and La_3Al_{11}[10] are two binaries related to the $BaAl_4$ structure type.[11] Figure 2 shows the

(5) Stoe. *X-Shape: Crystal Optimization for Numerical Absorption Correction*; Stoe & Cie Gmbh: Darmstadt, Germany, 1996.
(6) Petricek, V.; Dusek, M. *The crystallographic computing system JANA2000*; Institute of Physics, Praha, Czech Republic, 2000.
(7) Altomare, A.; Burla, M. C.; Camalli, M.; Cascarano, G.; Giacovazzo, C.; Guagliardi, A.; Moliterni, A. G. G.; Polidori, G.; Spagna, R. Sir97: a new tool for crystal structure determination and refinement. *J. Appl. Crystallogr.* **1998**, *32*, 115−119.
(8) Cordier, G.; Dietrich, C.; Friedrich, T. *Z. Kristall.* **1996**, *211*, 627−8.
(9) Zalutskii, I. I.; Kripyakevich, P. I. *Dopov. Akad. Nauk. Ukr. RSR Ser. A* **1967**, *29* (4), 362−6.
(10) Gomes de Mesquita, A. H.; Buschow Kurt, H. J. *Acta Crystallogr.* **1967**, *22* (4), 497−501.
(11) Andress, K. R.; Alberti, E. *Z. Metallk.* **1935**, *27*(6), 126−128.

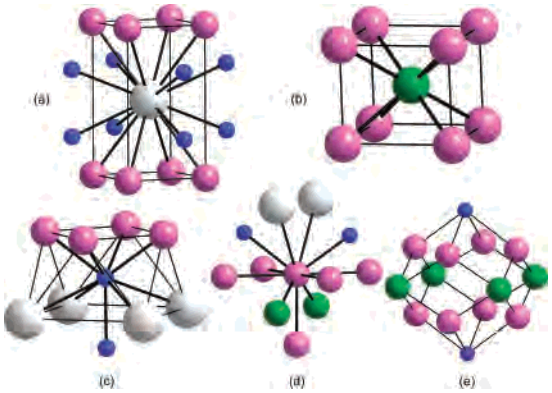

Figure 2. Representation of the different local environments (a) for La, (b) for Ni, (c) for the mixed Ni/Al site, (d) for Al, and (e) for the empty cavity at the center of the unit cell.

different local environments for each atom. La is surrounded by 8 Al and 8 mixed Ni/Al sites. It is interesting to notice that, on average, the amount of Ni and Al in the neighborhood of La, ~2 Ni atoms and ~14 Al atoms, is close to that in the vicinity of Ce in $Ce_4Ni_6Al_{23}$. Ni is in a slightly distorted cubic site of Al. The mixed site is coordinated by two squares formed, respectively, by 4 La atoms and 4 Al atoms. Finally, the Al atoms are in a pseudotetrahedral site of 2 Ni and 2 mixed sites (~2.5 Å) capped by 5 Al and also 2 La (~2.7−2.9 Å). Figure 2e illustrates the vacant RD site that we have already discussed. To our knowledge this structure type is not present in other La/Ni/Al compounds, although some structural analogues (RD sites, tetragonal structure) are observed with some RE/Ni/Ga and RE/Co/Ga compounds such as $LaNi_{0.6}Ga_6$, $HoCoGa_5$, $Ce_4Ni_2Ga_{20}$, $Ce_4Ni_2Ga_{17}$, Ce_4NiGa_{18}, and $Ce_3Ni_2Ga_{15}$.[12−14]

Moreover, this new structure is quite interesting, first, because it exhibits a large cavity (R~1.35 Å if we consider the metallic radii for Ni and Al) that may be filled by small atoms. Our chemical analysis as well as our X-ray single crystal refinement confirmed the lack of oxygen in the center of the RD site. Regarding hydrogen, EDXS measurements and X-ray refinements are not so helpful, although our experimental procedures sought to minimize the amount of impurities. A second point of interest is a relatively short distance between the two mixed sites (2.375 Å), which may be considered as a dimer. If we compare this distance to other Ni−Ni or Al−Al distances known in the literature, this one seems quite small. However, such short distances are observed in the analogous gallide compounds which possess Ga−Ga dimers (For example Ga−Ga=2.292 Å in Ce_4NiGa_{18} or 2.306 Å in $Ce_3Ni_2Ga_{15}$.). Nevertheless, larger Ni−Al distances are observed in the Gd/Ni/Al system. Indeed, in $GdNiAl_2$ and $GdNi_4Al$ the bond distances between Ni and Al are 2.45 and 2.48 Å, respectively.

This dimer and the Ni/Al ratio may play a role in the stability of this phase. Indeed, numerous syntheses under the same conditions to obtain different Ni/Al ratios for the mixed site were attempted, but as yet none has given another Ni/Al ratio. For the isostructural compounds $EuAu_2Ga_5$ and $SrAu_2Ga_5$[8] the authors, in fact, refined the compositions to be $EuAu_{1.86}Ga_{5.14}$ and $SrAu_{1.96}Ga_{5.04}$, with mixing of Au and Ga also occurring on the 2h site. However, since the results of their refinement give R-values of ca. 0.15, the Au/Ga ratio in these compounds needs to be confirmed.

Electronic Structure Calculations

To understand the stability of this phase, band structure calculations have been carried out using TB-LMTO and EHT electronic band structure calculations. Using TB-LMTO, we have studied two hypothetical models with supercells close to the refined structure with an ordering of Al and Ni on the mixed site.

Computational Details. TB-LMTO electronic band structure calculations were carried out in the atomic sphere approximation using the LMTO47 program.[15] Exchange and correlation were treated in a local spin density approximation.[16] All relativistic effects except spin−orbit coupling were taken into account using a scalar relativistic approximation.[17]

In the atomic sphere approximation, space is filled with small overlapping Wigner-Seitz (WS) atomic spheres. The symmetry of the potential is considered spherical inside each WS sphere, and a combined correction is used to take into account the overlapping part.[18] The radii of the WS spheres were obtained by requiring that the overlapping potential be the best possible approximation to the full potential and were determined by an automatic procedure.[18] This overlap should not be too large because the error in the kinetic energy introduced by the combined correction is proportional to the fourth power of the relative sphere overlap. Interatomic space was filled with one empty sphere (ES) at the center of the RD site by an automatic procedure[15] since the structure of the compound under examination is not densely packed. The WS radii of Ni and Al atoms are nearly equal (1.35 Å $< r_{Ni} <$1.38 and 1.33 Å $< r_{Al} <$1.38 Å), while the WS radius of La is 2.30 Å and the empty sphere has a radius of 1.37 Å.

The basis set included 6*s*, 5*d*, and 4*f* orbitals for La, 4*s*, 4*p*, and 3*d* orbitals for Ni, and 3*s* and 3*p* orbitals for Al. For the ES *s*, *p*, and *d* orbitals are used. The La-6*p* orbital, Al-3*d* orbital, and the ES *p* and *d* orbitals were treated by the Löwdin downfolding technique.[18] The **k**-space integrations were performed by the tetrahedron method. The self-consistent charge density was obtained using 64 irreducible **k**-points in the Brillouin zone for the tetragonal cell. The contribution of the nonspherical part of the charge density to the potential was neglected. The Fermi level was selected as the energy reference.

$La_4Ni_{1.5}Al_{5.5}$. To perform band structure calculations on $LaNi_{1+x}Al_{6-x}$ ($x = 0.44$) two different models have been studied which are necessarily approximations to the actual arrangement. Since the Ni/Al ratio of the mixed site refines close to 25/75, ordering of the Ni and Al atoms has been created in a cell four times larger along the *c* axis. Note that no additional superstructure reflections have been observed in any X-ray diffraction experiments, which means that Ni and Al are not ordered. Nevertheless, such orderings correspond to the closest structural approximations with the formulation $LaNi_{1.5}Al_{5.5}$. Model 1 contains 2 Ni-Al dimers

(12) Andersen, O. K. *Phys. Rev. B* **1975**, *12*, 3060−3083.
(13) Andersen, O. K.; Jepsen, O. *Phys. Rev. Lett.* **1984**, *53*, 2571−2574.
(14) Andersen, O. K.; Jepsen, O.; Glötzel, D. In *Highlights of condensed-matter theory*; Bassani, F., Fumi, F., Tosi, M. P., Eds.; New York, North-Holland, Lambrecht, W. R. L., 1985.
(15) Andersen, O. K. *Phys. Rev. B* **1986**, *34*, 2439−2449.
(16) Andersen, O. K.; Jepsen, O. *Phys. Rev. Lett.* **1984**, *53*, 2571−2574.
(17) Andersen, O. K.; Jepsen, O.; Glötzel, D. In *Highlights of condensed-matter theory*; Bassani, F., Fumi, F., Tosi, M. P., Eds.; New York, North-Holland, Lambrecht, W. R. L., 1985.
(18) Andersen, O. K. *Phys. Rev. B* **1986**, *34*, 2439−2449.

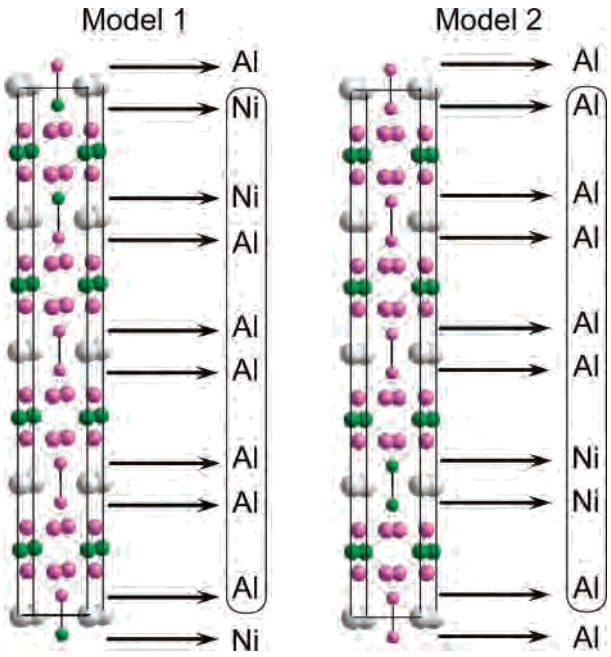

Figure 3. Representation of two unit cells of $LaNi_{1.5}Al_{5.5}$, model 1 and model 2 with two different orderings for the M−M dimers.

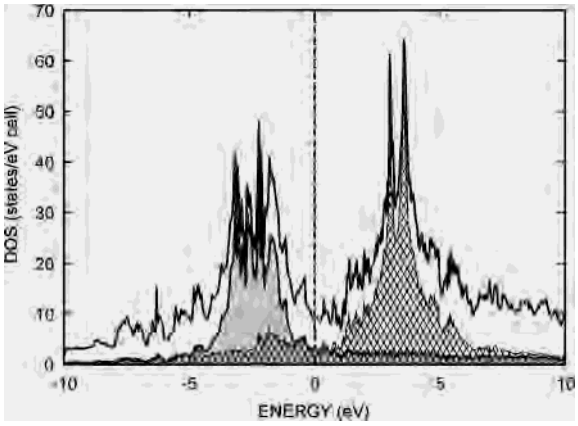

Figure 4. Total DOS end partial DOS calculated for $LaNi_{1.5}Al_{5.5}$. Gray DOS and hatched DOS correspond, respectively, to the Ni PDOS and La PDOS.

and 2 Al−Al dimers, whereas model 2 has 3 Al-Al dimers and 1 Ni−Ni dimer, as presented in Figure 3.

Band structure calculations were carried out on these two models under identical conditions (same size of the atomic spheres, same number and size of empty spheres). From the total energies of these two systems, model 1 is 4.5 eV more stable than model 2, which is rather significant even if the value of the total energy may be contested using the LMTO method. Such stabilization where heteronuclear dimers are preferred compared to homonuclear dimers has already been observed in other systems such as $Ln_3Au_2Al_9$.[19] The lower stability of model 2 relative to the model 1 may be understood as populating more antibonding Ni-*d* states in model 2. Thereafter, we will discuss only the band structure calculations of model 1 which is the more stable one.

Figure 4 illustrates the total DOS (TDOS) and some partial DOS (PDOS) 10 eV above and below the Fermi level, which

(19) Nordell, K. J.; Miller, G. J. *Angew. Chem.* **1997**, *36*(18), 2008−2010.

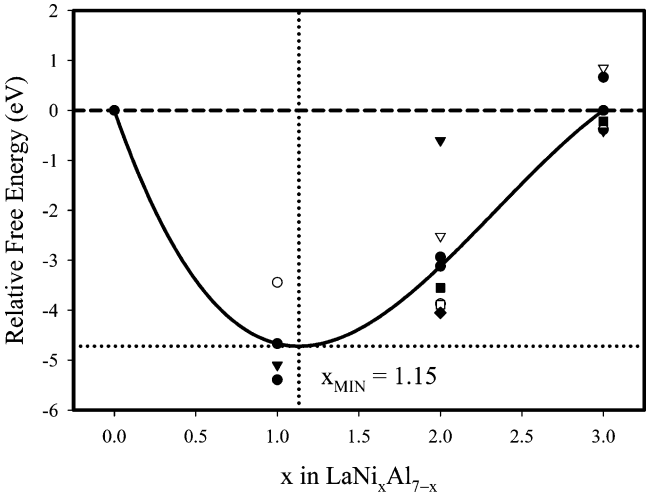

Figure 5. Plot of relative free energy vs Ni composition of $LaNi_xAl_{7-x}$. The relative energies for the different structural models are specifically shown, and the solid line is the polynomial fit to the weighted averages. The location of the minimum in this curve is noted by the dotted lines.

is chosen as the energy reference. The TDOS exhibits two broad peaks, one centered 3 eV below the Fermi level and the other one ca. 4 eV above the Fermi level. The first peak is mostly due to contributions from Ni-3*d* orbitals, whereas the other corresponds to the La-5*d* orbitals. However, we notice some La-5*d* states as well as some Al-3*p* states (none plotted) in the same energy window as the Ni-3*d* states, which means that electronic interactions occur between Ni-3*d*, La-5*d*, and Al-3*p* orbitals.

The DOS for $LaNi_{1.5}Al_{5.5}$ indicates that the Ni 3*d* band is mostly filled, 0.8 eV below the Fermi level. From our LMTO calculations, the *d*−*d* repulsions contribute to the observed composition, which can be demonstrated by a plot of the approximate free energy vs Ni composition (see Figure 5). We carried out semiempirical Extended Hückel calculations on different models of $LaNi_xAl_{7-x}$ for x ranging from 0 to 3. The experimental unit cell and atomic parameters from $LaNi_{1.45}Al_{5.55}$ were used for all models. All calculations utilized the tight-binding approximation with overlaps considered through second nearest neighbor cells. Total valence electron energies were evaluated by averaging the results of 500 k-points in the irreducible wedge of primitive cell in reciprocal space. Valence atomic orbitals for Ni (4*s*, 4*p*, and 3*d*) and for Al (3*s* and 3*p*) were used. For nonzero x, there are various ways of decorating the electronegative network with Ni and Al atoms. Those structures maximizing Ni−Ni separations lead to the lowest energy structures. Furthermore, for $x = 1$, these calculations give the lowest energy for Ni in the 1*b* Wyckoff site, which agrees with the experimental observations. For $x = 2$, the next preferred site is the 2h site, which is partially occupied in $LaNi_{1.45}Al_{5.55}$. The plot in Figure 4 illustrates the specific energies of the various models relative to the line connecting the weighted average values for $x = 0$ and $x = 3$ phases. The curve is a polynomial fit to the weighted average energies. The point on this curve where the slope is zero (x_{MIN}) marks the region ($x \leq x_{MIN}$) which is thermodynamically stable (with respect to these calculations) relative to the endpoints. This minimum occurs at $x_{MIN} = 1.15$, which is in reasonable agreement with

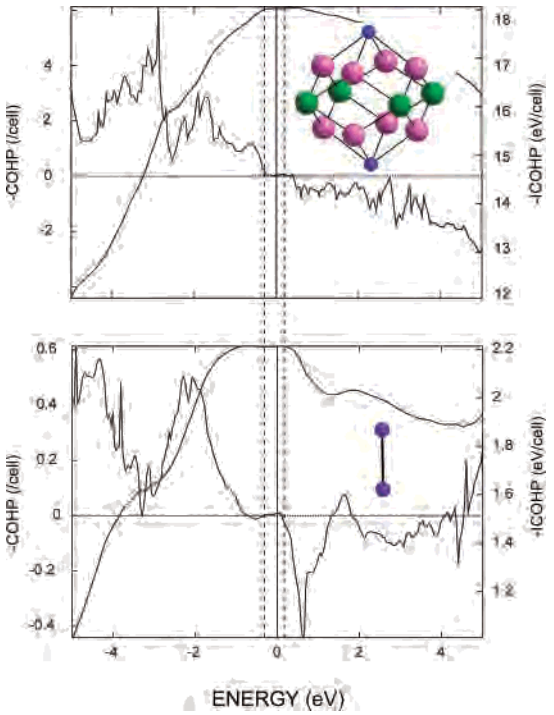

Figure 6. COHP curves of the (Ni.Al) framework (a) in the RD site and (b) in the dimer.

experiment, but whose value is limited by the nature of the approximations. Nevertheless, this plot demonstrates that the curvature of the graph of total energy of $LaNi_xAl_{7-x}$ vs Ni composition x will place an upper limit on the Ni composition between 1 and 2. This curvature arises primarily from the repulsions created by filled 3*d* bands of the Ni atoms in this intermetallic system.

To elucidate the nature of the interactions and especially those in the Ni−Al framework, COHP analyses have been performed. Figure 6 presents the −COHP curves, which show the interactions in the RD site as well as within the short dimers (d=2.375 Å), which connect two RD sites along the c axis. The −COHP values of the four RD sites and four dimers have been added since the real model is an average of this ordered model.

The Fermi level corresponds, in both cases, to the optimization of bonding interactions as bonding states are populated, whereas the antibonding states remain empty. These COHP results are consistent with recent investigations of "polar intermetallics"[20,21] and comparable to our observations in the Ce−Ni−Al system.[1] The origin of the stability of $LaNi_{1.44}Al_{5.56}$ may be explained by such optimized bonding in the Al−Ni framework. However, we also notice that surrounding the Fermi level (between −0.2 eV and +0.2 eV represented as dashed lines), the states are mostly nonbonding which means that in a rigid band approximation we can postulate small homogeneity width of composition from $LaNi_{1.40}Al_{5.60}$ to $LaNi_{1.58}Al_{5.42}$. So far, we have not identified other compositions for $LaNi_{1+x}Al_{6-x}$ than $x = 0.44$, which may indicate that the rigid band approximation is not valid for this example. Indeed, by changing the composition we may also change the atomic distances, especially in the dimer, which may modify the nature of the interactions as well as the shape of the DOS and the COHP. COHPs of the La−Al interactions have also been performed but not shown. These COHPs are similar to the ones observed for $Ce_4Ni_6Al_{23}$.[1] Indeed, the crossing point between the bonding and antibonding states is rather close to the Fermi level although some La−(Ni,Al) bonding states are still unpopulated.

"$LaNiAl_6$" and "$LaNi_3Al_4$": The Rigid Band Model. As mentioned before we have identified just a single composition $LaNi_{1+x}Al_{6-x}$ ($x = 0.44$) which demands mixed occupation of Ni and Al in the dimer site. However, "$LaNiAl_6$" (Al−Al dimer) and "$LaNi_3Al_4$" (Ni−Ni dimer) are two pleasant hypothetical compounds to examine theoretically, especially with respect to the rigid band model. Since we do not expect the same external parameters (cell parameters, volume, and c/a ratio) and internal parameters (atomic positions) for these examples as for $LaNi_{1.44}Al_{5.56}$, we performed calculations to optimize the hypothetical cells. Starting from the parameters obtained for $LaNi_{1.44}Al_{5.56}$, we first optimize the volume to 150 Å^3, then the c/a ratio to 2.09. These optimizations for $LaNiAl_6$ show an increasing volume and elongation of the tetragonal cell compared to those for $LaNi_{1.44}Al_{5.56}$. Thereafter, we have optimized the two internal parameters: the z coordinates of the Al and the X sites. To summarize, all these optimizations are in accordance to what were expected since an increase of Al concentration implies an increase of the cell volume as well as an increase of the distance of the Al−Al dimer to 2.55 Å. Such optimizations have also been performed for "$LaNi_3Al_4$" (Ni−Ni dimer) where we observe a decrease of the volume as well as a decrease of the Ni−Ni dimer distance to 2.32 Å. These optimizations also justify the postulate previously discussed that a rigid band model is delicate in these compounds, since a change of composition is immediately accompanied by a change of the structural parameters.

Finally, starting from the optimized internal and external parameters we calculated the DOS of the two hypothetical compounds as shown in Figure 7. The TDOS and the Ni−PDOS, in gray, are superimposed. In both cases the Fermi level is close to a pseudogap as seen in models 1 and 2. However it is not as clearly evident as in $LaNi_{1.5}Al_{5.5}$, especially in the Ni rich case, "$LaNi_3Al_4$", which shows a broader Ni-3*d* block with a tail in the DOS at the Fermi level. This tail consists of mostly antibonding states coming from σ interactions in the Ni−Ni dimer as shown in the inset by an electron density map in the vicinity of the Ni−Ni dimer. The antibonding character of these states justifies the relative instability of Ni rich compounds in the pseudosolid solution $LaNi_{1+x}Al_{6-x}$. These two calculations also confirm that a rigid band model is not totally appropriate. The stability of the structure and composition of $LaNi_{1+x}Al_{6-x}$ corresponds to a fine compromise between dealing with Ni−Ni antibonding interactions and the Ni amount in the dimer in order

(20) Häussermann, U.; Amerioun, S.; Eriksson, L.; Lee, C.-S.; Miller, G. J. *J. Am. Chem. Soc*. **2002**, *124*, 4371−4383.
(21) Miller, G. J.; Lee, C.-S.; Choe, W. In *Inorganic Chemistry Highlights*; Meyer, G., Naumann, D., Wesemann, L., Ed.; Wiley-VCH: Berlin, 2002; pp 21−53.

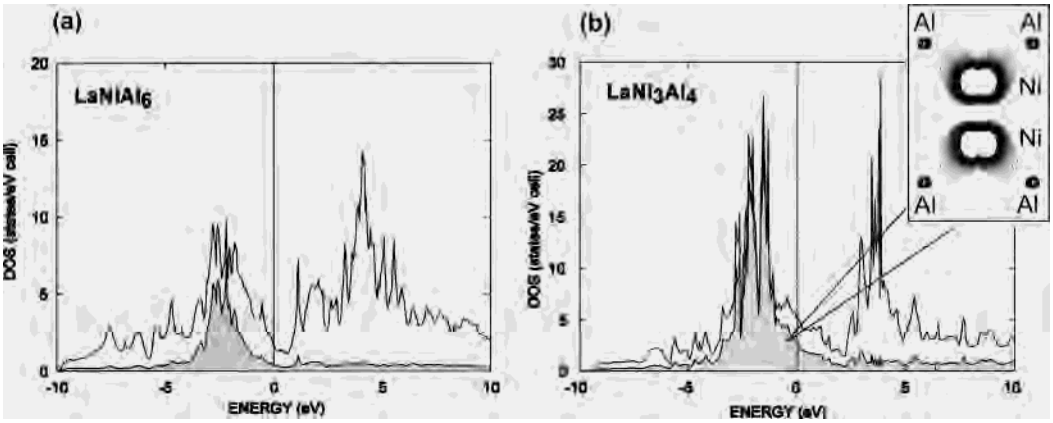

Figure 7. TDOS and Ni−PDOS (in gray) for the optimized hypothetical compounds (a) "$LaNiAl_6$" and (b) "$LaNi_3Al_4$". The inset of the "$LaNi_3Al_4$" DOS shows an electron density map in the vicinity of the Ni−Ni dimer, indicating the antibonding character of the states just below the Fermi level.

to provide a certain number of valence electrons to the formula unit. However, we may postulate that other compositions may exist probably toward lower Ni concentrations.

Summary

A new compound in the La−Ni−Al system, $LaNi_{1+x}Al_{6-x}$ ($x = 0.44$), has been synthesized and its structure refined by X-ray diffraction. This new structure is quite interesting since it is closely related to the $BaAl_4$ structure type but with an open cavity in the center of the unit cell. Moreover, band structure calculations using density functional theory demonstrate optimized Al−Al and Ni−Al bonding, which may explain the relative stability of $LaNi_{1.44}Al_{5.56}$ and confirm our recent investigations of "polar intermetallics" in other systems such as the Ce−Ni−Al system. Using the same idea, we may understand the stability of $EuAu_{1.86}Ga_{5.14}$ and $SrAu_{1.96}Ga_{5.04}$ obtained by Cordier et al.[8] since these compounds have approximately the same number of valence electrons per formula (19.28 and 19.08 electrons, respectively) as $LaNi_{1.44}Al_{5.56}$ (19.68 electrons). This relation between the structure type and the number of electrons may help us to target different compositions in other intermetallic systems.

Finally, our work shows that a rigid band model is not appropriate in that system and eventually explains the limitation to find other nearby phases with other Ni/Al ratios.

Acknowledgment. This work was supported by the NSF DMR 99-81766 and DMR 02-41092. The authors are grateful to Warren Straszheim of the Materials Analysis Research Laboratory of Iowa State University for running Energy-Dispersive X-ray Spectroscopy measurements on our samples.

Supporting Information Available: X-ray crystallographic file in CIF format for the structure determination of $LaNi_{1+x}Al_{6-x}$ ($x = 0.44$). This material is available free of charge via Internet at http://pubs.acs.org.

IC0497331